Time-resolved observation of the Eigen cation in liquid water

Wafa Amir, Guilhem Gallot, François Hache, S. Bratos, J.-C. Leicknam, R. Vuilleumier

Time-resolved observation of the Eigen cation in liquid water

Wafa Amir, Guilhem Gallot, François Hache, S. Bratos, J.-C. Leicknam, and R. Vuilleumier

Citation: The Journal of Chemical Physics **126**, 034511 (2007); doi: 10.1063/1.2428299
View online: http://dx.doi.org/10.1063/1.2428299
View Table of Contents: http://scitation.aip.org/content/aip/journal/jcp/126/3?ver=pdfcov
Published by the AIP Publishing

Time-resolved observation of the Eigen cation in liquid water

Wafa Amir,[a] Guilhem Gallot,[b] and François Hache
Laboratoire d'Optique et Biosciences, Ecole Polytechnique, CNRS, INSERM, 91128 Palaiseau, France

S. Bratos, J.-C. Leicknam, and R. Vuilleumier
Laboratoire de Physique Théorique des Liquides, Université Pierre et Marie Curie, 4 Place Jussieu, 75252 Paris Cedex 05, France

(Received 23 June 2006; accepted 5 December 2006; published online 18 January 2007)

Experimental observation and time relaxation measurement of the hydrated proton Eigen form $[H_3O^+(H_2O)_3]$ are presented here. Vibrational time-resolved spectroscopy is used with an original method of investigating the proton excess in water. The anharmonicity of the time-resolved spectra is characteristic of the Eigen-type proton geometry. Proton relaxation occurs in less than 200 fs. A calculation of the potential energy confirms the experimental result and the Eigen cation lifetime is in good agreement with previous molecular dynamics simulations. © *2007 American Institute of Physics*. [DOI: 10.1063/1.2428299]

I. INTRODUCTION

Water is a key element in chemistry and biochemistry and its study is of increasing interest to a large scientific community. In particular, water is the most universal solvent and its role is critical for the chemistry of life. It possesses many puzzling characteristics including the proton mobility which is at least five times larger than for other cations.[1,2] This anomalous high mobility plays a dominant role in the acid-base and proton transfer reactions which occur in many important biochemical processes. However, the abnormal proton high mobility in water is still an open question.[3,4] In particular, the apparent displacement of proton in water is too rapid to be due to an atomic displacement. A possible explanation of this feature was first suggested by von Grotthuss[5] in the 19th century. He proposed a mechanism where the charge, and not the proton itself, is transferred between water molecules. Description of this so-called Grotthuss mechanism involves two limit forms of proton: a proton delocalized between two adjacent water molecules ($H_5O_2^+$, Zundel type) and a proton localized on a water molecule $[H_3O^+(H_2O)_3$, Eigen type].[6] Infrared experiments and simulations of proton in hydrated crystals as well as in small water clusters confirm the existence of the two limit types.[7–9] Extension to solution is not easy, since an infinite number of configurations exist in liquid water. Nevertheless, the fast proton mobility has been thoroughly investigated in the liquid phase by computer simulation techniques and molecular dynamics simulations.[10–13] In liquid water, the proton does not exchange between two precise water geometries but between two wide classes of water environments. In the following, we keep the Eigen and Zundel limit structural motifs in analogy to the symmetry of the two classes of proton-water geometries. Most interestingly, it appears that the vibrational energy of the different forms of the hydrated proton $H^+(H_2O)_n$ is not uniformly distributed, enabling hole burning pump-probe experiments. Recent neutron diffraction[14] and x-ray absorption[15] measurements studied the modification of the hydrogen bonding network in the presence of proton in solution and point out the observation of Eigen and Zundel structural motifs. However, direct experimental evidence of these forms in liquids is very difficult to obtain. Very recently, a femtosecond pump-probe experiment studied high concentration solutions of proton in liquid water,[16] confirming the ultrafast relaxation processes in the Grotthuss mechanism. Two reasons can explain the difficulty of experimental observation. On the one hand, simulations show that the proton can jump from one form to the other one on a subpicosecond time scale and it is therefore difficult to isolate either form. On the other hand, even if one form is isolated, the determination of the limit form involved is difficult. Spectroscopic data on the two forms are only known from simulations which reveal that the ion absorption structures are very broad presumably due to ultrafast spectral diffusion. In this article, we demonstrate experimental observation of the Eigen-type limiting form of proton in water using femtosecond time-resolved vibrational spectroscopy. First, the use of ultrashort pulses allows us to excite a definite species and follow its evolution before relaxation or conversion. Second, it gives access to the excited-state absorption spectrum which will be critical for excited proton form identification.

We carry out time-resolved experiment on a binary mixture HCl/H_2O in the 2600–3000 cm^{-1} range, using low proton concentration (below 1M) to avoid Coulombic interaction between protons, contrary to a previous study.[16] According to molecular dynamics simulation, this spectral range corresponds to the Eigen-type absorption.[17] By measuring the excited species absorption spectrum and comparing it with model quantum calculation, we confirm that we observe the Eigen cation. This direct experimental observation of this proton type provides important information on its dynamics. In Sec. II, our experimental method for obtaining

[a]Present address: Colorado School of Mines Physics Department, 1523 Illinois St., Golden, CO 80401.
[b]Author to whom correspondence should be addressed. Electronic mail: guilhem.gallot@polytechnique.fr

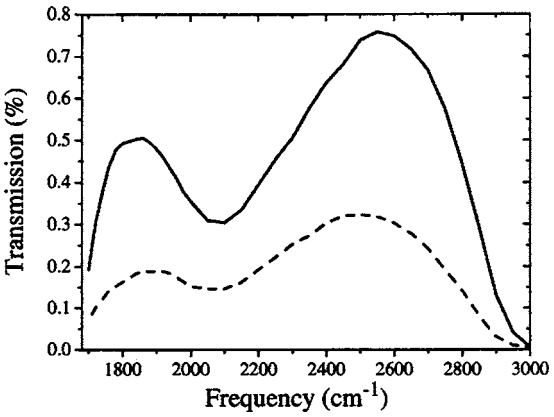

FIG. 1. Transmission spectra through 40 μm of pure water (solid line) and 0.5*M* HCl/H_2O (dashed line).

the hydrated proton spectrum is described. In particular, the technique of extracting proton information from the water background is thoroughly discussed. Finally, in Sec. III, we present the main experimental results and discuss about the proton spectrum relaxation.

II. FEMTOSECOND VIBRATIONAL SPECTROSCOPY OF HYDRATED PROTON

A. Experimental setup and procedure

To perform pump-probe hole burning experiments in the midinfrared range, energetic laser pulses are required. The central element of the infrared laser source we used is a titanium-sapphire amplifier, delivering 130 fs pulses at 800 nm with a repetition rate of 1 kHz. It drives two lines of pulses independently tunable in the midinfrared. The principle of the pulse generation is parametric amplification of a quasicontinuum in the near infrared, followed by frequency mixing in the midinfrared.[18] The features of the source are as follows. The pump pulses have a duration of 150 fs and a spectral width of 65 cm^{-1}. It delivers more than 10 μJ in the 2800–3800 cm^{-1} range. The independently tunable weaker line (the probe) has similar characteristics but with a maximum energy smaller than the pump energy by one order of magnitude. The time delay between the pump and the probe is precisely controlled by a computer. The sample cell is 40 μm thick and contains pure water or a solution of HCl in water at room temperature. Typical transmission of pure water and 0.5*M* HCl in water is presented in Fig. 1 and shows the important modification of spectral absorption in the presence of the hydrated proton. The sample is circulated to avoid heating problems. The pump and the probe beams are focused in the sample by two 25 mm focal length calcium fluoride lenses. The angle between the pump and the probe beams is 15°. In order to reduce the noise, the probe signal is normalized by a signal tap off the cell. Furthermore, the pump beam is chopped at half the repetition rate of the laser (i.e., 500 Hz), in order to obtain a probe signal with and without the pump. Using this procedure, we achieve a signal to noise ratio of 10^4. For a given pump frequency, differential spectra are recorded by tuning the probe frequency for several pump-probe time delays. Typical transmission changes of 10^{-3} are measured. For each probe wavelength,

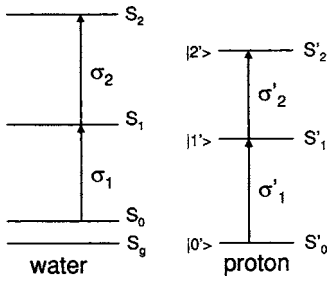

FIG. 2. Energy diagrams for pure water and for solvated proton, with the corresponding cross sections.

we measure the time-resolved differential absorption in pure water and in the HCl solution. This is necessary because pure water gives a large differential signal in this frequency range. This feature has been thoroughly studied recently.[19] It is therefore important to be able to extract the signal of the HCl/H_2O solution from the background due to water. Such an extraction is not straightforward and requires a careful understanding of the origin of the signal in this binary mixture. The purpose of the following section is to analyze this question and to come out with a "normalization factor" enabling us to isolate the relevant signal from the experiment.

B. Calculation of pump-probe signal in binary H_2O/HCl mixture

The fundamental difficulty in the study of the proton signature in water is that pure water already exhibits a pump-probe signal, even without proton. Therefore, the system has to be carefully analyzed to suppress the background signal of pure water from the signal measured with the protonated mixture. The following calculations take into account the unusual vibrational properties of pure water in this spectral domain,[19] where librational mode plays a major role. Pure water can be described using a four-level quantum system (see Fig. 2 and Ref. 19). Pumping it around 2800 cm^{-1} initiates a transition from the librational state S_0 to the first vibrational excited state S_1. From S_1, three transitions are possible: to the ground state ($S_1 \rightarrow S_g$, bleaching), to the second excited state ($S_1 \rightarrow S_2$, induced absorption), or back to the librational state ($S_1 \rightarrow S_0$, bleaching). The ν_{OH} frequency being equal to 3250 cm^{-1}, the role of the $S_1 \rightarrow S_g$ transition is totally negligible, and the ground level S_g will be neglected in the following. The plan of our paper is as follows. First, a simple analytical model describing the HCl/H_2O binary mixture will be presented, using the above assumptions based on the properties of pure water. Next, this simple model will be validated using full rate equation modeling.

1. Simple analytical model

In this model, the water molecule H_2O as well as the ion $(H_3O)^+$ are both assimilated to a three-level quantum system (Fig. 2). Their total numbers per unit volume are N and N', respectively. The absorption cross sections are σ_1, σ_2, σ'_1, and σ'_2. Cross sections related to the proton naturally include the contribution of the surrounding water molecules since they belong by definition to the hydrated proton entity. At the submolar HCl concentrations used in the experiments, the

change of the optical dielectric constant is negligible and does not alter the measurements of the cross sections of the hydrated proton. The sample has a thickness L. The assumption of a weak pump flux ϕ is made. It corresponds to typical experimental conditions and one can assume that $\sigma_1\phi \ll 1$ and $\sigma_1'\phi \ll 1$. In the absence of the pump excitation, the transmitted photon flux ϕ_p is given by the Beer-Lambert equation

$$\phi_p(z) = \phi_0 e^{-(N\sigma_1 + N'\sigma_1')z}. \tag{2.1}$$

The pump excitation modifies the populations of different quantum states. The transmitted photon flux for the probe beam is then

$$\phi_{pp} = \phi_0 \exp\left\{\int_0^L \{-[N - \Delta N(z)]\sigma_1 + \Delta N(z)\sigma_1 - \Delta N(z)\sigma_2\}dz\right\} \times \exp\left\{\int_0^L \{-[N' - \Delta N'(z)]\sigma_1' + \Delta N'(z)\sigma_1' - \Delta N'(z)\sigma_2'\}dz\right\}, \tag{2.2}$$

where ΔN and $\Delta N'$ designate the number of molecules having left the ground state for the first excited state. The measured differential pump-probe transmission $T_{pp} = \phi_{pp}/\phi_p$ is then

$$T_{pp} = \frac{T_{\text{probe}}}{T_0} = \exp\int_0^L [2\Delta N(z)\sigma_1 - \Delta N(z)\sigma_2]dz \times \exp\int_0^L [2\Delta N'(z)\sigma_1' - \Delta N'(z)\sigma_2']dz. \tag{2.3}$$

Let $\Delta\sigma = \sigma_2 - 2\sigma_1$ and $\Delta\sigma' = \sigma_2' - 2\sigma_1'$. One obtains

$$T_{pp} = \exp\int_0^L -[\Delta\sigma\Delta N(z) + \Delta\sigma'\Delta N'(z)]dz. \tag{2.4}$$

The experimental challenge is then to extract the solute cross section $\Delta\sigma'$ from the total signal. At this point the following assumption is made. One assumes that the ratio $\alpha = \Delta N'(z)/\Delta N(z)$ remains constant during propagation through the sample. This implies that the excited populations of the solvent and solute are created in a similar way by the pump. This will be true as long as there is no saturation effect. Validity of this assumption will be numerically discussed later on. Note that $\int_0^L (\Delta N + \Delta N')dz$ is the total number of excited molecules contained in a cylinder having a basis of 1 m^2 and a length L. This number is equal to the variation of the pump flux $\phi(0) - \phi(L) = \Delta\phi$. Then

$$\int_0^L (\Delta N + \Delta N')dz = (1+\alpha)\int_0^L \Delta N dz = \Delta\phi. \tag{2.5}$$

Therefore,

$$\int_0^L (\Delta N\Delta\sigma + \Delta N'\Delta\sigma')dz = (\Delta\sigma + \alpha\Delta\sigma')\int_0^L \Delta N dz \tag{2.6}$$

$$= (\Delta\sigma + \alpha\Delta\sigma')\frac{1}{1+\alpha}\Delta\phi. \tag{2.7}$$

Equation (2.3) then yields

$$T_{pp} = \exp\left[-(\Delta\sigma + \alpha\Delta\sigma')\frac{1}{1+\alpha}\Delta\phi\right]. \tag{2.8}$$

Similarly, in the case of pure solvent, i.e., with $\alpha = 0$, the relative probe transmission is given by

$$T_{pp}^w = \frac{T_{\text{probe}}^w}{T_0^w} = e^{-\Delta\sigma\Delta\phi^w}. \tag{2.9}$$

The differential signals measured in the experiments for the binary solute/solvent and pure solvent are related to these quantities by

$$R = 1 - T_{pp}, \qquad R^w = 1 - T_{pp}^w. \tag{2.10}$$

Since relative transmission changes are small, one can develop these expressions into

$$R = (\Delta\sigma + \alpha\Delta\sigma')(\Delta\phi/1) + \alpha, \qquad R^w = \Delta\sigma\Delta\phi^w. \tag{2.11}$$

We now define a normalization parameter κ by

$$\kappa = \frac{\Delta\phi}{\Delta\phi^w}\frac{1}{1+\alpha}, \tag{2.12}$$

from which the relative transmissions of the solvent and solute may be obtained. There results

$$S = R - \kappa R^w = \frac{\alpha\Delta\phi}{1+\alpha}\Delta\sigma'. \tag{2.13}$$

This normalization parameter accounts for the absorption of the solute in the binary mixture: photons absorbed by the solute do not contribute to the solvent excitation, implying that the solvent contribution is less in the binary mixture than in the pure solvent. Under the assumption of a weak pump, the parameter α can be obtained from the linear spectra of H_2O and H_{aq}^+. Since $\Delta N(z) = N\sigma_1\phi$ and $\Delta N'(z) = N'\sigma_1'\phi$, $\alpha = N'\sigma_1'/N\sigma_1$, which can be obtained from linear absorption measurements at 2800 cm^{-1}, since the linear transmissions for H_2O and H_{aq}^+ are

$$T_{H_2O}^{(l)} = e^{-N\sigma_1 L}, \qquad T_{H_{aq}^+}^{(l)} = e^{-N\sigma_1 L}e^{-N'\sigma_1' L}. \tag{2.14}$$

The important point of this calculation is that this normalization parameter can be easily obtained from linear

transmission data at the frequency of the pump in the solvent and in the binary mixture. It is not affected by the physical evolution of the system after excitation and is therefore a robust normalization parameter. In our experimental conditions, the parameter κ is equal to 0.7. The normalization allows the extraction of $\Delta\sigma' = \sigma_2' - 2\sigma_1'$, which is the only parameter depending on the probe frequency and which provides the nonlinear pump-probe response of the solute, as in an isolated three-level system.

2. A full three-level quantum system simulation

The above simple model shows that a normalization is possible if the ratio α defined as $\Delta N'(z)/\Delta N(z)$ remains constant. We shall now consider a full simulation of the quantum systems, precisely taking into account the excited populations for both solvent and solute, and see if normalization is still possible. If α is not constant, then

$$R = \Delta\sigma \int_0^L \Delta N(z)dz + \Delta\sigma' \int_0^L \Delta N'(z)dz,$$
$$R^w = \Delta\sigma \Delta\phi^w, \tag{2.15}$$

from which a new normalization parameter κ' is obtained:

$$\kappa' = \frac{\int_0^L \Delta N dz}{\Delta\phi}. \tag{2.16}$$

However, κ' depends on how the population evolves, and it is difficult to evaluate. The question is to know whether, under realistic conditions, the previously defined parameter κ is a good approximation to κ'. Full rate equations for solvent populations are given by

$$\frac{\partial N_0}{\partial t} = (N_1 - N_0)\sigma_1 F(z,t),$$
$$\frac{\partial N_1}{\partial t} = (N_0 - N_1)\sigma_1 F(z,t) + (N_2 - N_1)\sigma_2 F(z,t), \tag{2.17}$$

and for solute populations

$$\frac{\partial N_0'}{\partial t} = (N_1' - N_0')\sigma_1' F(z,t),$$
$$\frac{\partial N_1'}{\partial t} = (N_0' - N_1')\sigma_1' F(z,t) + (N_2' - N_1')\sigma_2' F(z,t). \tag{2.18}$$

Temporal features of the pump now have to be taken into account to fully simulate saturation during pump propagation. Due to the small thickness of the experimental sample, the pump profile remains constant throughout the propagation. Experimental pump pulses are Gaussian, and the temporal profile is

$$F(t) = \sqrt{\frac{4\ln 2}{\pi\Delta\tau^2}}\phi \exp\left(-4\ln 2 \frac{t^2}{\Delta\tau^2}\right), \tag{2.19}$$

where $\phi = \int_{-\infty}^{+\infty} F(t)dt$ and $\Delta\tau$ is the full width at half maximum of the pulse.

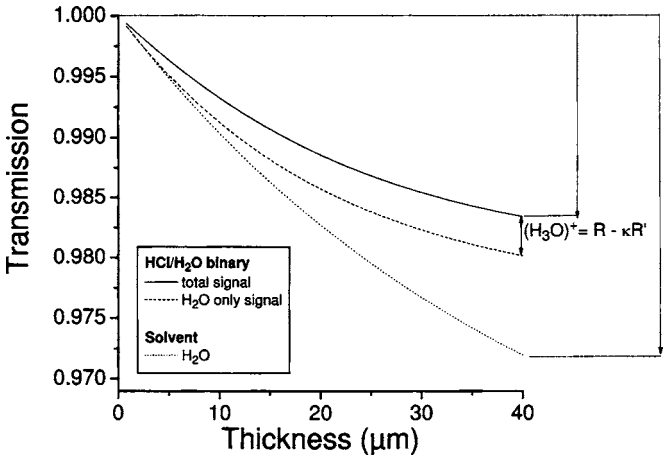

FIG. 3. Normalization of binary $(H_3O)^+/H_2O$ mixtures. Relative probe transmissions are shown vs propagation depth in the sample for binary mixture and pure solvent. Solid line: total signal for binary mixture; dashed line: water contribution to the mixture signal; dotted line: pure solvent. The real contribution from solute can be extracted by normalizing the binary and pure solvent relative transmissions, using normalization coefficient κ.

The sample is divided into sections of small thickness. For each section, Eqs. (2.17)–(2.19) are numerically solved to give the resulting population distribution. The energy of the pump is corrected for absorption; then one shifts to the next section. At the end of the simulation, the whole evolution of the populations is known. A typical result is shown in Fig. 3, which presents the evolution of the relative transmission of the probe versus the depth of propagation for binary mixture and pure solvent. From the population evolution, one can calculate the evolution of α versus z, as given by Fig. 4. Cross sections for pure water are taken from previous work.[19] Cross sections for solute come from the experimental data. Figures 3 and 4 are calculated for a solute concentration of 1% in the number of molecules of hydrated proton with respect to the number of water molecules (0.5M). Figure 4 shows the evolution of α with two pump fluxes, respectively, 1×10^{17} and 5×10^{17} photons/cm^2. It appears that for high flux, α is not constant anymore throughout propagation, which means that evaluation of normalization from linear data is no longer possible. On the contrary, for lower flux, α is almost constant, and the difference between

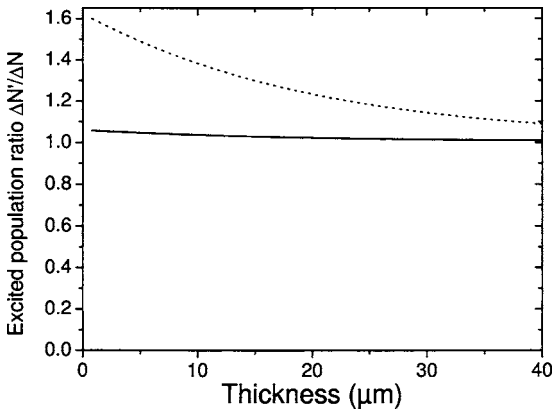

FIG. 4. Excited population ratio $\Delta N'/\Delta N$ vs propagation distance for two pump fluxes at 5×10^{17} (dotted line) and 10^{17} (solid line) photons/ cm^2.

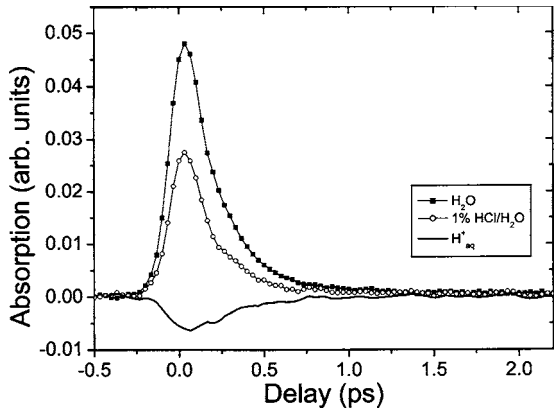

FIG. 5. Differential absorption of HCl (0.5M) and H_2O as a function of the pump-probe delay. The pump and probe frequencies are fixed at 2800 cm^{-1}. The proton signal (dotted curve), extracted with a normalization coefficient (κ=0.7), displays a bleaching behavior.

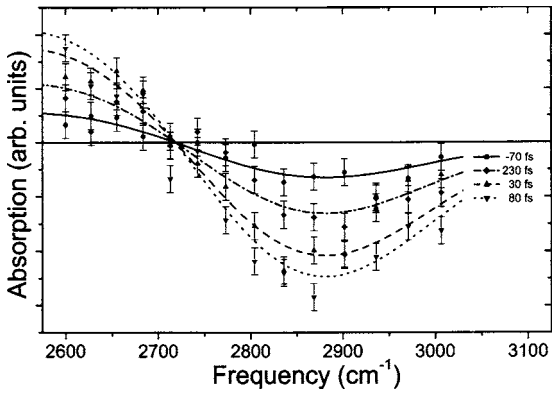

FIG. 6. Time-resolved spectra of the hydrated proton in liquid water. The dots represent experimental data with the pump frequency at 2800 cm^{-1} for various pump-probe delays (−70, 30, 80, and 230 fs).

κ and κ' is very small, less than 1%, and will not affect the quality of the normalization. Pump energy then has to remain under an upper limit, which corresponds to differential probe absorptions below 5%. In our experiments, this condition is fully satisfied and we can safely use the above-defined normalization parameter κ.

III. EXPERIMENTAL RESULTS AND DISCUSSION

The differential absorption signals obtained for pump and probe frequencies tuned at 2800 cm^{-1} are displayed in Fig. 5 for pure water and HCl solution (0.5M). The similarity between the two signals is a clear indication of the importance of the above-mentioned calculation: most of the solution signal comes from the excited-state absorption in water that was discussed in Ref. 19. To investigate the possible role played by the counterion Cl^-, we also recorded differential spectra of NaCl solutions with the same concentration. No measurable difference with respect to pure water has been observed, showing that the presence of the proton is fully responsible for the spectral features of HCl in solution. In order to extract the proton contribution, we apply Eq. (2.13) and obtain a neat bleaching of the proton absorption. It is clear from the shape of these curves that the excited state is short lived. However, at that point it is hazardous to try to extract any information because population relaxation, spectral diffusion, and laser pulse duration are intricate in this time-resolved signal. This point will be discussed further when the whole spectral response is examined. Similar treatment has been performed for 14 probe wavelengths in the 2600–3050 cm^{-1} range and yielded absorption bleaching on the high-energy side whereas it yielded excited-state absorption on the low-energy one. These findings are summarized in Fig. 6 where the time-resolved spectra of the hydrated proton are displayed for four significant delays: −70, 30, 80, and 230 fs. Several pieces of information can be extracted from these curves. First, all curves have the same shape, indicating that there is no observable spectral diffusion. This feature is consistent with an ultrafast spectral diffusion. Theoretical studies indicate spectral diffusion of hydrated proton to be much faster than the one in pure water, which is less than 1 ps. It is then probable that such spectral diffusion effects take place on a rapid time scale not accessible to the experiment. Note that such very rapid energy redistribution has been observed in pure water.[19,20] Second, this spectral shape with a low-energy excited-state absorption and a high-energy bleaching is characteristic of three-level quantum systems displaying a *negative* anharmonicity, that is to say that the first excited-state absorption is redshifted compared to the ground state one. As discussed below, this feature is a signature of Eigen-type proton. Finally, we can extract from these spectra a more precise information on the relaxation time of the excited proton. For that, we begin with fitting the induced-absorption structures with Gaussian functions and then plot the band areas as a function of time. The result is displayed in Fig. 7. Because the band areas are directly connected to the density of excited protons, this curve allows one to extract the population relaxation time despite the band shifts. By applying the procedure exposed in Ref. 21, it is possible to get rid of the pulse duration and to extract the genuine relaxation time. Since no evidence of measurable spectral relaxation is found within the experimental time resolution, the time domain pump-probe data should evolve with the same time scale as frequency domain evolution. An average of time evolution data is then shown in Fig. 7 and

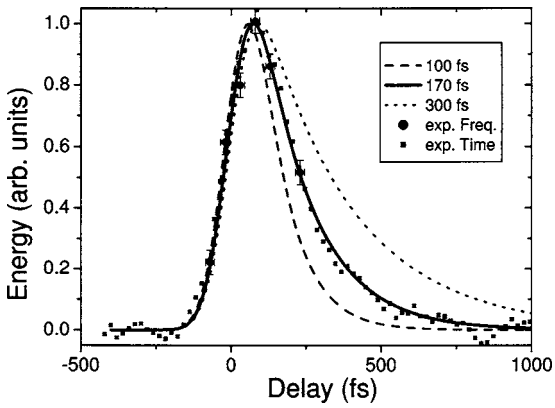

FIG. 7. Energy relaxation of the excited proton. The round dots are deduced from Gaussian fits of the experimental data. The square dots originate from the averaging of three time domain pump-probe experiments, with probe frequency at 2750, 2800, and 2850 cm^{-1}. The lines are calculations for different relaxation times.

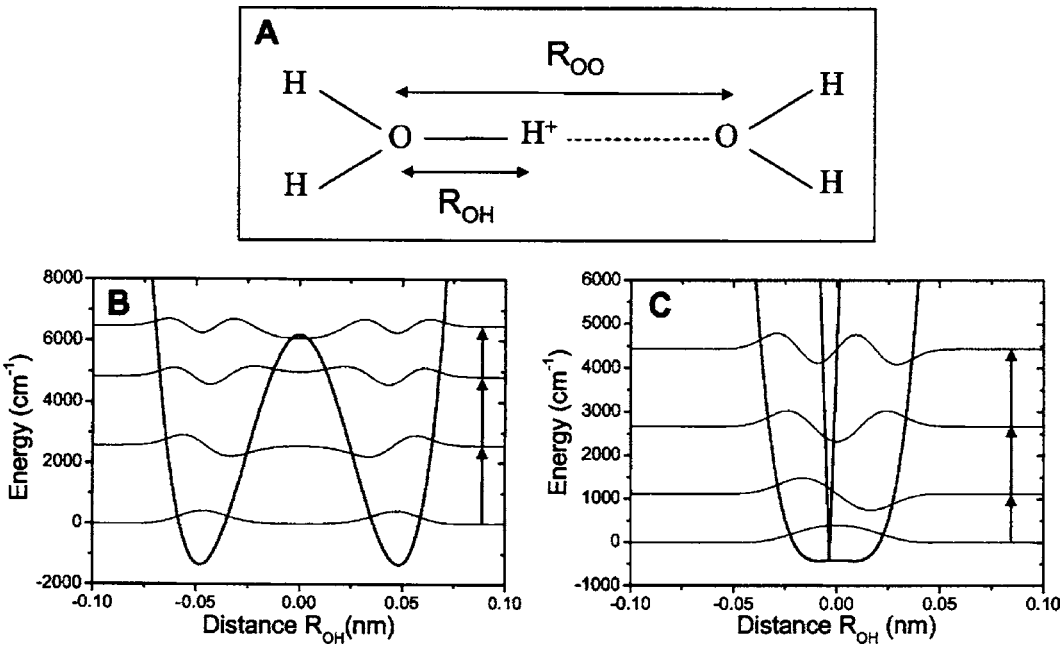

FIG. 8. (A)Geometry of the proton between two water molecules. [(B) and (C)] Potential energy and energy levels for the Eigen [(B) R_{OO}=0.3 nm] and Zundel [(C) R_{OO}=0.26 nm] ions. The reaction coordinate is the oxygen-hydrogen distance R_{O-H}. The Eigen ion transforms into the Zundel ion by reducing R_{O-O}. Anharmonicity is negative in the Eigen form and positive in the Zundel form.

provides a better fitting precision at longer delays. The lines in Fig. 7 are fits obtained with this procedure and yield a decay time of 170±20 fs. Given the low density of proton in the solution, excitation transfer to other protons is not likely to happen. This fast relaxation of the proton vibration is probably due to an efficient coupling with the vibrational modes of the nearby water molecules. These conclusions are in good agreement, within experimental uncertainty, with previous work by Woutersen and Bakker[16] and confirm the validity of our normalization procedure. Contrary to this work, we cannot observe a spectral component of the Eigen-type proton at higher frequency, since pure water strongly absorbs above 3100 cm^{-1}.

We now come to the discussion of the negative anharmonicity observed in Fig. 6. In order to understand the signature of the two proton types (Eigen or Zundel) in terms of anharmonicity, we have developed a simple quantum calculation aimed at evaluating the energy potential surface of a hydrated proton interacting with a water molecule (see Fig. 8). For the sake of simplicity, we suppose that the three atoms O···H···O are aligned. The potential used in the calculation can be found in the literature.[11,22] It is issued from an extended quantized empirical valence-bond model for describing the dynamics of an excess proton in water clusters and liquid water,[23] validated from *ab initio* and density functional theory calculation. It is well suited for the characterization of the shape of the potential undergone by the proton. The extended model includes all the possible valence states accessible to the excess proton at a given time step and allows for a consistent description of the delocalized electronic structure around the excess charge. The potential consists of two parts: an intramolecular potential which accounts for the H_3O^+ molecule and an intermolecular one which deals with the interaction between H_3O^+ and H_2O.[23] The parameters can be found in Ref. 22. The potential surface of the proton is calculated as a function of the distance R_{OH} together with the corresponding quantum levels, whose variations are analyzed when changing the distance between the two oxygen atoms, R_{OO}. The results are summarized in Fig. 8: when the two oxygen atoms are far apart (typically $R_{OO}>0.3$ nm), the proton tends to get localized on one oxygen atom (Eigen type). The localized proton then moves in a sharp potential well. On the contrary, when the two oxygen atoms are closer ($R_{OO}<0.26$ nm), the potential well is much flatter and the proton wave function is completely delocalized between the two oxygen atoms, which corresponds to the Zundel type. In order to address this point more quantitatively, we have carried out quantum mechanical calculation of the first and second stretching mode frequencies by solving a one-dimensional Schrödinger equation for the O–H coordinate R_{OH} using the potential previously developed and the numerical Numerov method.[24] The striking point is that, looking closer at the energy levels, the anharmonicity is negative in the Eigen case, whereas it is positive in the Zundel case. Our experimental finding of a negative anharmonicity therefore allows us to conclude that it is the Eigen proton that we have observed and demonstrated in our time-resolved experiment. Note that this conclusion is in agreement with theoretical calculations which predicted that it is the Eigen type which preferentially absorbs at 2800 cm^{-1}.[17]

IV. CONCLUSION

In this article, we have investigated the ultrafast dynamics of proton in pure water by performing femtosecond pump-probe experiment in the 2600–3000 cm^{-1} range. This study requires a thorough knowledge of the behavior of water in this frequency range,[19] and the ability to achieve ul-

trashort time resolution in this mid-IR range. It permits to monitor the proton in a definite Eigen type before it converts into the Zundel type. We thus observed the excited proton with a relaxation time of 170 fs. Assigning it to the Eigen type was inferred from the negative anharmonicity which is characteristic of the localized form of the proton. This experiment should contribute to the elucidation of the von Grotthuss mechanism fundamentals.

[1] P. W. Atkins, *Physical Chemistry* (Oxford University Press, Oxford, 1997).
[2] N. Agmon, J. Phys. Chem. A **109**, 13 (2004).
[3] N. Agmon, Chem. Phys. Lett. **244**, 456 (1995).
[4] J. T. Hynes, Nature (London) **397**, 565 (1999).
[5] C. J. D. von Grotthuss, Annales de Chimie **58**, 54 (1806).
[6] D. Marx, M. E. Tuckerman, J. Hutter, and M. Parrinello, Nature (London) **397**, 601 (1999).
[7] J.-W. Shin, N. I. Hammer, E. G. Diken, M. A. Johnson, R. S. Walters, T. D. Jaeger, M. A. Duncan, R. A. Christie, and K. D. Jordan, Science **304**, 1137 (2004).
[8] M. Miyazaki, A. Fujii, T. Ebata, and N. Mikami, Science **304**, 1134 (2004).
[9] J. M. Headrick, E. G. Diken, R. S. Walters, N. I. Hammer, R. A. Christie, J. Cui, E. M. Myshakin, M. A. Duncan, M. A. Johnson, and K. D. Jordan, Science **308**, 1765 (2005).
[10] D. Wei and D. R. Salahub, J. Chem. Phys. **101**, 7633 (1994).
[11] R. Vuilleumier and D. Borgis, J. Chem. Phys. **111**, 4251 (1999).
[12] S. Izvekov and G. A. Voth, J. Chem. Phys. **123**, 044505 (2005).
[13] U. W. Schmidt and G. A. Voth, J. Chem. Phys. **111**, 9361 (1999).
[14] A. Botti, F. Bruni, S. Imberti, M. A. Ricci, and A. K. Soper, J. Chem. Phys. **121**, 7840 (2004).
[15] M. Cavalleri, L.-A. Näslund, D. C. Edwards, P. Wernet, H. Ogasawara, S. Myneni, L. Ojamäe, M. Odelius, A. Nilsson, and L. G. M. Pettersson, J. Chem. Phys. **124**, 194508 (2006).
[16] S. Woutersen and H. J. Bakker, Phys. Rev. Lett. **96**, 138305 (2006).
[17] J. Kim, U. W. Schmidt, J. A. Gruetzmacher, G. A. Voth, and N. E. Scherer, J. Chem. Phys. **116**, 737 (2002).
[18] G. M. Gale, G. Gallot, F. Hache, and R. Sander, Opt. Lett. **22**, 1253 (1997).
[19] W. Amir, G. Gallot, and F. Hache, J. Chem. Phys. **121**, 7908 (2004).
[20] M. L. Cowan, B. D. Bruner, N. Huse, J. R. Dwyer, B. Chugh, E. T. J. Nibbering, T. Elsaesser, and R. J. D. Miller, Nature (London) **434**, 199 (2005).
[21] S. Bratos and J.-C. Leicknam, J. Chem. Phys. **103**, 4887 (1995).
[22] R. Vuilleumier and D. Borgis, J. Phys. Chem. B **102**, 4261 (1998).
[23] R. Vuilleumier and D. Borgis, Chem. Phys. Lett. **284**, 71 (1998).
[24] G. Dahlquist and A. Bjorck, *Numerical Methods* (Dover, Mineola, NY, 2003).